Supercritical carbonation of calcareous composites: influence of mix design

Elham Farahi [a, b], Phil Purnell [c], Neil R Short [d]

a. Formerly School of Engineering, University of Warwick, Coventry CV4 7AL, UK.

b. Present address: AMEC, 601 Faraday Street, Birchwood Park, Birchwood

Warrington,WA3 6GN, UK. +44 1925 675489, elham.farahi@amec.com

c. Corresponding author: Institute for Resilient Infrastructure, School of Civil

Engineering, University of Leeds, Leeds LS2 9TJ, UK. +44 113 343 0370,

p.purnell@leeds.ac.uk

d. Formerly School of Engineering and Applied Science, Aston University, Birmingham

B4 7ET, UK.

Abstract

This work combined compression moulding with subsequent super-critical carbonation treatment (100 bar, 60°C, 24 h) to fabricate cement and/or lime based ceramic composites with various aggregates. Composites were examined using mechanical testing, XRD, He pycnometry and thin-section petrography. Composites with lime-only binders were significantly weaker than those with cement-lime binders regardless of the degree of carbonation. Flexural strengths in excess of 10 MPa were routinely achieved in large (>100 mm) specimens. Aggregate type (calcareous vs siliceous) had a significant effect on the microstructure and properties of the composites. Calcareous aggregates appear to augment the strength enhancement effected during super-critical carbonation by encouraging preferential precipitation of calcite at the binder-aggregate interface.

Keywords

Super-critical carbonation; mechanical processing; lime; cement; flexural testing; petrography

1. Introduction

1

Calcareous composites based on Portland cement and lime (such as concrete, mortar, fibre-reinforced cements etc) are naturally prone to carbonation when exposed to atmospheric air. The reaction involves carbon dioxide and calcium bearing compounds within the hydrated phase of the matrix, transforming it into an intimately interconnected matrix of calcium carbonate ($CaCO_3$) and hydrous silica and/or alumina gel. For lime mortars, carbon dioxide diffuses into the capillary pores of the mortar matrix and combines with water, forming weak carbonic acid (H_2CO_3). This acid dissociates into carbonate (CO_3^{-2}) and hydrogen (H^+) ions which then react with portlandite ($Ca(OH)_2$) to produce calcium carbonate [1-3].

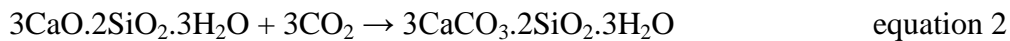$$Ca(OH)_2 + CO_2 \rightarrow CaCO_3 + H_2O + Heat \quad \text{Equation 1.}$$
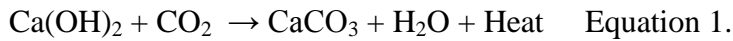
Carbonation acts as the primary mechanism of cementation in lime-based composites, transforming the packed assemblage of portlandite crystals into an interlocking mass of calcium carbonate. In cement composites however, CO_2 reacts with portlandite, any unhydrated cement (mainly $3CaO.SiO_2$ and $2CaO.SiO$; in cement chemistry notation C_3S and C_2S respectively), calcium silicate hydrates (C-S-H) and residual sodium and potassium ions in the pore solution of the cement matrix, forming insoluble calcium carbonate crystals precipitated in the available spaces within the matrix pore network, hydrated silica (as a result of decalcification of the C-S-H gel), as well as few other minor products including sodium and potassium carbonates and decalcified aluminate hydrates [4-8].

The rate and extent of carbonation in a cementitious matrix mainly depends on the chemical and microstructural nature of the cement hydration products, as well as the various factors which affect the diffusivity and reactivity of CO_2 in the hardened cement paste. Carbonation under atmospheric conditions is very slow, mainly due to the low partial pressure of CO_2 in the atmosphere (about 0.03 – 0.06 % v/v) and the resultant slow rate of diffusion of CO_2 into the structure of a lime or cement based matrix [6,9]. It may thus take many decades for full carbonation to develop across the entire depth of a concrete component.

2

The crystallization and precipitation of the calcium carbonate during the cement carbonation process was described by Garcia-Gonzalez et al as a three step mechanism [7,8]: (1) Dissolution of calcium ions from calcium-bearing phases, (2) absorption of carbon dioxide and development of carbonate ions, (3) chemical reaction, nucleation and crystal growth.

The process can be approximately summarised by the following main four reactions [9-11]:

$3CaO.2SiO_2.3H_2O + 3CO_2 \rightarrow 3CaCO_3.2SiO_2.3H_2O$ equation 2

$Ca(OH)_2 + CO_2 \rightarrow CaCO_3 + H_2O$ equation 3

$3CaCO_3.2SiO_2 + 3\ CO_2 + \mu H_2O \rightarrow 2SiO_2.\mu H_2O + CaCO_3$ equation 4

$2CaCO_3.2SiO_2 + 2CO_2 + \mu H_2O \rightarrow 2SiO_2.\ \mu H_2O + 2CaCO_3$ equation 5

Carbonation causes a significant drop in the hydroxide concentrations of the pore solution and lowers its pH, from ~12.5-13.5 down to about 9 in the fully carbonated zone. The exact pH will depend on the HCO_3/CO_3 equilibria, which in turn will be controlled by both the degree of carbonation and amount of alkalis (NaOH, KOH) present [4,12,13]. In the case of steel reinforced concrete structures, a significant drop in pH will destroy the passive oxide film protecting the reinforcement, potentially leading to corrosion of reinforcement and deterioration of structural components if oxygen and water are available [4,13]. However, this drop of pH and simultaneous removal of CH from the matrix could be beneficial with regards to alternative concrete reinforcement products such as glass and plastic fibres in the cementitious matrix, which in normal conditions may suffer from alkali and/or calcium hydroxide induced durability issues [10,14,15].

The carbonation process also alters the microstructure of calcareous based composites. As the molecular volume of calcium carbonate (calcite) is 11.2% greater than that of calcium hydroxide, the deterioration/ decalcification of C-S-H- gel and precipitation of calcium carbonate crystals during carbonation will result in filling up of the pores with

3

small tightly packed crystals of calcite [6,13]. As the bulk volume of the solid does not change significantly, this increase in volume will be accommodated within the matrix by filling previously empty pores and capillaries, reducing the total pore volume, pore size and thus permeability of the cementitious based composite [4]. These alterations in the pore structure will have a direct influence on enhancing the strength (compressive and flexural) of carbonated cementitious based matrix [2,7,8,13,16].

As a consequence, one area that has attracted much interest amongst research communities is the application of supercritical carbon dioxide ($scCO_2$) technology for rapid carbonation of cementitious based products to enhance their mechanical and microstructural properties. The process involves exposing cementitious materials to CO_2 at elevated temperature and pressure (> 31ºC and 71 bar). At these conditions, CO_2 enters the supercritical region where it possesses the properties of both gaseous (diffusivity and viscosity) and liquid (density and activity) CO_2. These properties make $scCO_2$ an excellent medium for carbonating cementitious composites very quickly. Under supercritical conditions, CO_2 diffuses very fast into the interior of the cementitious sample causing carbonation to occur throughout the pore structure [7, 8, 17].

Compared with atmospheric or sub-critical accelerated carbonation, super-critical carbonation conditions greatly accelerate the rate of reaction, reducing completion times from years to hours. This has been claimed by some to be mainly due to the significant rise of CO_2 solubility in the pore water, combined with the ease of penetration and rapid diffusion of a large amount of $scCO_2$ into the cement paste pore network [7, 8]. Atmospheric carbonation has been defined as a CO_2 diffusion controlled process where carbonation progresses from the exterior to interior pores of cement matrix at a rate which is proportional to the square root of time [8,11]. Supercritical carbonation however is not diffusion controlled. It has been observed in several studies [7,8,17] that $scCO_2$ diffuses very quickly into the interior of the samples causing carbonation to occur throughout the pore structure; further increasing the temperature and pressure of $scCO_2$ does not significantly increase the degree of carbonation [7,8,11,17,18].

4

Domingo *et al.* [19] showed that under scCO$_2$ conditions, the rate of crystallisation and precipitation of calcite was much faster compared with natural carbonation, as the concentration of CO$_3$ $^{-2}$ ions in the matrix pore solution was significantly higher [19]. The calcite precipitated by the process was better developed and more crystalline in nature than the calcite developed during atmospheric carbonation, resulting in development of a more interconnected microstructure. This exhibited both lower overall porosity and a higher proportion of porosity attributed to gel pores, which consequently resulted in higher mechanical strength [7,8].

The effect of scCO$_2$ on cementitious materials was initially investigated by the oil industry in the context of conditions encountered in deep CO$_2$-enhanced oil and gas recovery walls [20]. However, its use as a treatment to improve the properties of cementitious composites was first initiated by Jones and was patented in the USA in the late 1990s [21]. Since then, several researchers have demonstrated the advantages of treating either wet or hardened cement paste with scCO$_2$ to produce fully carbonated cement matrices, either as monoliths or reinforced with glass fibres with improved mechanical and chemical properties. A wide range of cementitious materials can be rapidly carbonated to almost uniform carbonate content throughout the depth of the treated samples with a resultant matrix having an almost neutral pH [6,7,8,10,11,14,15,22,23].

Investigations intended to remedy the durability problems formerly associated with glass fibre reinforced cement (GRC) indicated that compared with non-carbonated controls, super critically carbonated GRC samples exhibited a significant increase in matrix strength, design toughness, matrix/fibre bond strength, dimensional stability and improvement in resistance to age-embrittlement [10,14,15,22,23]. SCC treatment also enhanced the mechanical properties and dimensional stability of plain (non-reinforced) cementitious based materials. It was observed that compared to uncarbonated or even naturally carbonated specimens, SCC treated samples exhibited much greater resistance to swelling and shrinkage after they were exposed to number of different environments. This was attributed to the significant modifications in their pore structure, having

5

reduction in total porosity and exhibiting higher pore volume being attributed to gel pores of less than 10nm,after exposure to $scCO_2$ [23]. The change in strength and porosity of SCC-treated cementitious materials was also studied by Garcia-Gonzalez et al [7, 8] and Purnell *et al.* [14] and it was shown that SCC treatment reduced the total porosity of cement based composites by up to a factor of $\sim 2 - 3$ and eliminates the coarse capillary porosity (pores larger than 30nm) that is ubiquitous to the structure of normal cement paste [15].

1.1. Aims and objectives.

The aim of this work was to investigate the potential of combining novel forming methods (suited to mass producing high quality cementitious composites) with supercritical carbonation processing to permit the manufacture of high-value technical ceramic components whilst avoiding traditional manufacturing and long term moist curing processes. The novel forming technique reported here was compression moulding combined with vacuum dewatering (adopted from plastic and polymer parts manufacturing industries) to fabricate "green "specimens. Here the term "green" is associated with specimens that have been compression moulded but not cured or hardened, exhibiting only "sand-castle" strength, capable of supporting their self weight during storage prior to further treatment. The objectives were focused on optimization of the mix design and manufacturing conditions to produce green specimens with quality surface finish and structural integrity that would also become fully carbonated after being exposed to the supercritical carbonation (SCC) process, and exhibit significant enhancement in structural and micro structural properties.

2. Experimental methods

2.1. Materials

Binders used were combinations of hydrated lime, [L, Limbux Extra, Buxton Lime/Tarmac, UK] with $Ca(OH)_2$ content of >96%, and ordinary Portland cement [C, CEM1, Buxton Lime/Tarmac, UK]. Aggregates [A] were combinations of silica sand [S,

Buxton Lime/Tarmac, UK], crushed limestone (2.36 mm to dust fraction) [CL, Buxton Lime/Tarmac, UK] and a silica aggregate (SA) which was deliberately engineered to have the same particle size distribution as CL (i.e. 99:66:45:33:20% mass passing through sieve sizes 2.36:1.81:0.60:0.30:0.15 mm respectively).

2.2. Sample manufacturing

The designed compression moulding tool as shown in Figure 1, comprised two 300×170 mm parts, capable of producing six samples at a time, each 170mm long with a trapezoidal cross sectional shape 22/34mm wide × 17mm deep. The trapezoidal shape was developed from several prototypes to combine ease of demoulding and practicality of performing flexural bending tests.

To process the green forms, the tool was fixed into a compression moulding machine design for processing thermoplastics. Cementitious mix (manufactured to a constant relative workability, monitored using a modified slump test) was fed to the mould and laid in the base between two layers of filter papers; the sample was the pressed for varying times and pressures. To allow removal of excess water from the cementitious mix during pressing, a series of 2 mm diameter holes at 10 mm centres were incorporated along the base and upper part of the tool. Excess water was squeezed out and removed through the filter papers via the vacuum manifold connected to the holes. The applied pressure was then released and the green specimens immediately demoulded.

[Figure 1]

Figure 1: Compression moulding tool.

To investigate the amount of water lost by the manufacturing process, the weight of specimens before and immediately after demoulding was recorded. For each mix design, a batch of 8 green samples were manufactured; 3 were used as "control", 3 for exposure

7

to SCC treatment and 2 which were immediately oven dried to measure the total water content

2.3. Pre-treatment conditioning

After pressing, green specimens were conditioned by drying the samples in a fan oven for 12 h at 25°C to remove 70 – 75% of the free water, previous work having shown that this was optimal with regards to facilitating the carbonation treatment [14,15].

2.4. Treated (carbonated) samples

The SCC treatment was performed by exposing the conditioned samples to static, water saturated $scCO_2$ at 60°C, 10 MPa for 24 h in a 5.5 litre stainless steel reaction vessel as detailed in Figure 2, having internal dimensions of ø100 × 500 mm. The inside temperature was maintained by a jacket circulating water around the vessel from a water bath that is attached to the vessel. The temperature inside the vessel was monitored by a thermocouple attached to inside of the pressure vessel. The requisite CO_2 pressure in the vessel was generated by allowing a predetermined mass of solid CO_2 ('dry ice') to decompose within the sealed vessel and equilibrium was reached after about 25min. To reach 10 MPa pressure while the inside temperature is set at 60°C, 1.7kg of dry ice was required.

[Figure 2]

Figure 2: Photo and diagram illustrating the $scCO_2$ reaction vessel

2.4. Control Samples

After pre-carbonation conditioning, control samples were stored sealed at room temperature for a similar period (i.e. 24hr, as per SCC treatment) before mechanical testing. These samples were thus only partially hydrated.

8

2.5. Mechanical Testing

Triplicate specimens were tested for flexural strength using a fully articulated 4-point bending fixture attached to a screw controlled mechanical testing apparatus (Testometric Micro 100KN PCX) with a major span of 145 mm and a minor span of 45 mm. All testing was performed at a constant cross head displacement of 1 mm min^{-1}. Mid span deflection was measured using an integrated LVDT type transducer. The machine was controlled by computer software which captured all load – displacement data with 0.1 N and 1 µm resolution up to failure. Flexural strength at failure (modulus of rupture) was calculated using standard beam theory. Both treated and control samples were in total ~40 hours old when tested.

2.6. Chemical Analysis

Immediately after mechanical testing, the degree of carbonation of treated specimens was analysed using X-ray Diffraction (XRD, Philips PW 1830). Small portions were removed from each specimen and finely ground to pass a 150 µm sieve. The analysis was then performed using CuKα radiation between 15° and 80° 2θ at 0.6° min^{-1} (0.02°, 2 s per step). For each mix design, triplicate control and carbonated specimens were tested and degree of carbonation was examined semi-quantitatively by using ratio of peak height of three most prominent peaks for portlandite and alite (C_3S) for three control and three carbonated samples.

2.7. Helium Pycnometry

Remnants from the mechanical tests were used to determine total porosity using helium pycnometry. For each case, $10 \times 13 \times 20$ mm cuboids were cut from samples using a precision saw and dried by immersion in acetone for 48hr, followed by storage over silica gel until reaching constant weight (taking between 14 and 21 days) after the method described by Aligizaki [24]. The cuboids were then measured using a micrometer and the bulk density calculated. They were then tested in a helium pycnometer (AccuPyc 1330,

9

Micromeritics) over 10 purge cycles to provide the true densities, from which the porosity was calculated. For each case, 3 control and 3 carbonated specimens were prepared and tested.

2.8. Microstructural Analysis

Thin section petrography (TSP) was used to investigate the effect of $scCO_2$ on the microstructure of the cementitious composites. This is a useful method for examining the microstructure of a composite, especially when authoritative identification of phases (such as differentiation between CH and calcium carbonate) is required [24]. In this work, standard 28×48 mm $\times$ 30 μm thick, clear resin impregnated thin sections were prepared, with the final grinding being performed using a non-aqueous medium to avoid distortion of soluble phases.

3. Results and discussion

3.1 Preliminary optimisation of green processing

To determine the optimum pressing conditions, the effect of pressing time and pressure on strength of green specimens both immediately after demoulding and after 24hr exposure to $scCO_2$ was investigated. A range of forming pressures (4.5 MPa to 13.5 MPa) and pressing durations (1 min to 8 min) was investigated. Experiments were carried out using a mix design of 1.5C:0.5L:5A:1.1W with A= 65:35 CL:S, all proportions by mass). Although the pressing conditions had a marked effect on the green strength, they had a negligible effect on the strength of the treated samples (Figure 3) Within the range studied, pressing green forms under 9 MPa pressure and 1 min was found to be the most convenient pressing regime and therefore used throughout the rest of the work.

[Figure 3]

Figure 3: Processing parameters vs flexural strength. Left: green samples; right: carbonated samples. Legend = compression moulding pressure. Error bars = ± 1 st dev.

10

3.2. Influence of mix design – cement:lime ratio and aggregate:cement ratio.

Figure 4 shows the flexural strength of various samples before and after $scCO_2$ treatment and its variation with cement:lime ratio and aggregate:binder ratio. The aggregate combination in these samples was 35:65 CL:S by mass. This range of mix designs was chosen after preliminary work suggested that such samples were capable both of producing green forms with sufficient green strength and good surface finish that would also become fully carbonated after being exposed to supercritical carbonation (SCC) process.

[Figure 4]

Figure 4: Flexural strength vs. mix design. Aggregate = 35:65 S:CL. All proportion ratios by mass. Error bars = ± 1 st dev.

SCC treatment significantly enhanced the strength of all specimens, in some cases by over 500%. Flexural strength of treated samples increased markedly with C:L ratio. The optimum aggregate:binder ratio with regard to strength was around 2:1.

The compression process also resulted in reduction of the total water within the processed composite. [Table 1]

Table 1: The water content of the mix designs shown in Figure 4, both prior to and post pressing process.

shows the degree of water reduction within the manufactured green specimens (shown in Figure 4) associated with the compression moulding.

[Table 1]

11

Table 1: The water content of the mix designs shown in Figure 4, both prior to and post pressing process.

Figure 5 shows, for the same samples, the degree to which $Ca(OH)_2$ (in cement chemistry notation, CH) was depleted by the SCC treatment as measured semi- quantitatively by XRD using peaks at $2\theta = 18.1$ and $34.1°$. In samples with pure lime binders, or with high aggregate contents, CH was depleted by treatment to below the XRD detection limit; in other samples, CH was depleted by >90%. Analysis of XRD peaks at $2\theta = 32.07°$ and $32.33°$ showed that C_3S was always depleted to below the detection limit. This may suggest that unhydrated C_3S is more susceptible to supercritical carbonation than CH.

[Figure 5]

Figure 5: XRD analysis of CH depletion vs. mix design. Aggregate = 35:65 S:CL. All proportion ratios by mass. Error bars = ± 1 st dev.

Comparison between mechanical testing and XRD (Figures 4, 5) suggests little correlation between degree of carbonation and treated strength. In treated samples made with lime only matrices, strength was much lower than the comparable treated samples made from lime/cement binder (e.g. C:L:A of 0:0.5:1 cf. 0.5:0.5:2 having strength of 1.64 MPa cf. 9.22 MPa), despite full carbonation (i.e. complete depletion of CH). These results suggest that the binding ability of the carbonated C-S-H gel (i.e. silica gel which is formed both from decalcification of existing C-S-H gel during SCC treatment and formation of new gel phase during carbonation of C_3S) is far greater than that of interlocking calcium carbonated crystals alone. Formation of a gel phase appears to be essential to bind the particles within the carbonated structure together.

3.3. Influence of mix design - aggregate composition

To investigate the effect of changes in aggregate composition (i.e. ratios of sand to limestone or silica aggregate) experiments were carried out using C:L:A of 0.5:0.5:2 with 5 different aggregate compositions: 100% S, 65:35 S:CL, 65:35 S:SA, 35:65 S:CL and

12

35:65 S:SA. The SA was used in order to study the effect of changes in aggregate composition independently of any particle size effect.

Results (Figure 6) showed that despite the strength of control samples being similar for all 5 samples (varying between 1.62 – 1.98 MPa), the treated samples made with limestone aggregate were significantly stronger than those made with just sand or engineered silica aggregate. The effect became more marked as the limestone content increased. The strength of treated samples made from 35:65 S:CL was about 60% higher than those made with with 35:63 S:SA (9.32 MPa cf. 5.79 MPa), despite both aggregates having an identical PSD and limestone generally being considered a weaker aggregate than silica [25,26].

[Figure 6]

Figure 6: Flexural strength vs. aggregate composition. Mix design 0.5C:0.5L:2A . All proportion ratios by mass. Error bars = ± 1 st dev.

XRD results (Figure 7) indicated almost complete carbonation was achieved in all samples; CH depletion by the SCC process was generally more than 95%. In all samples, as before, C_3S was depleted to below the detection limit.

Figure 8 shows the porosity of control and carbonated samples for mix design 0.5C:0.5L:2A with aggregate types 65:35 CL:S & 65:35 SA:S. SCC treatment reduced the total porosity of the samples by ~40% regardless of the aggregate type. This reduction in total porosity was attributed to the decalcification process and precipitation of calcium carbonate into the macro and micro-pore structures. As the precipitated $CaCO_3$ has low solubility, it will fill the pore system and densify the cement paste [7,16]. Results also indicated that the total porosity of both control and treated samples made from CL was about 15% lower than that of SA contained samples. This correlates well with the mechanical testing results of treated samples for these mix designs (Figure 7). Since SA has the same PSD as CL and could reasonably be expected to consist of stronger individual particles, these findings suggest that the increased strength of samples containing CL is attributable to chemical, rather than physical, effects; the presence of

CL affects the formation of the carbonated solid phase assemblage during treatment in such a way as to promote low porosity and high strength.

[Figure 7]

Figure 7: XRD analysis of CH depletion vs. mix design. Mix design 0.5C:0.5L:2A. All proportion ratios by mass. Error bars = ± 1 st dev.

[Figure 8]

Figure 8: Porosity (via helium pycnometry) vs aggregate composition. Mix design 0.5C:0.5L:2A. All proportion ratios by mass. Error bars = ± 1 st dev.

3.4. Microstructural investigation- Thin Section Petrography

Figure 9 shows the microstructure of a control sample made from mix design 0.5C:0.5L:2A having aggregate combination of 65:35 CL:S. The groundmass (the material between the crystalline particles) appeared dark and amorphous owing to the poorly crystalline unhydrated cement minerals and some C-S-H gel, and was studded with bright flecks of small indistinct calcium hydroxide crystals {P}. The interface between the aggregate particles and the groundmass was not intimate, with voids evident along the matrix/aggregate interface. The porosity was high as there were not enough hydrated products (e.g. CH, C-S-H) at this relatively early stage (~1 day) of hydration to fill the internal spaces within matrix. This correlated well with the helium pycnometry. Similar microstructure was observed in control samples made from SA (Figure 10).

[Figure 9]

Figure 9: Thin section micrograph of control sample with crushed limestone aggregate (A = 65:35 CL:S). Horizontal field of view = 0.7 mm. Cross-polarised light. P = portlandite $Ca(OH)_2$

[Figure 10]

14

Figure 10: Thin section micrograph of control sample with silica aggregate (A = 65:35 SA:S). Details as figure 9.

Figure 11 shows the microstructure of the carbonated matrix made from aggregate combination 65:35 CL:S. The paste fraction was relatively featureless and the groundmass was much lighter than in the control sample, composed of cryptocrystalline calcium carbonate (identified by its high birefringence) mixed with an amorphous phase, presumably decalcified C-S-H gel. The dark inclusions represent non-crystalline materials, considered to be carbonated remnants of unhydrated cement grains that retain their original shape (pseudomorphs). This has been also observed by other investigators [14,15,27]. Compared to control samples, the structure is much denser and there is very little porosity at the matrix/aggregate interface. The interface between aggregate grain (especially CL grains) and the groundmass has been filled with carbonated products, causing the matrix to more closely and intimately follow the coastline of the aggregate grain.

[Figure 11]

Figure 11: Thin section micrograph of SCC treated sample with crushed limestone aggregate (A = 65:35 CL:S). Details as figure 9.

[Figure 12]

Figure 12: Thin section micrograph of SCC treated sample with silica aggregate (A = 65:35 SA:S). Details as figure 9.

A similar general microstructural arrangement was observed in carbonated samples made from SA (Figure 12). However, compared with SA, a significantly more intimate matrix/aggregate bond was evident between CL and the carbonated groundmass. In treated samples made with SA aggregate, the groundmass is not well bonded to the SA grain and there are still pores present at the matrix/aggregate interface; these interfacial pores are not present in treated samples made CL.

15

Figure 11 also shows cracks (caused by mechanical testing, not the carbonation process) running through the carbonated groundmass and passing "straight on" through the CL aggregate particle but around the quartz sand particles. In samples containing SA, cracks running through the carbonated groundmass disappear into the voids at matrix/aggregate interface. This suggests that in the CL samples, the interface has attained strength comparable to that of the limestone aggregate and the bond between the carbonated matrix and aggregate grain was strong and very intimate, while in the case of SA aggregate the interface between carbonated matrix and SA grains was weaker and less intimate. This correlated well with the flexural strength (Figure 6) and porosity (Figure 8) findings above.

It seems likely that the CL grains (composed of ~98% $CaCO_3$) were acting as a nucleation site for precipitation of the calcium carbonate during carbonation, which was therefore formed preferentially at the aggregate-matrix interface. Since this region is generally the most porous and thus weakest zone in cementitious composites [28], the effect on both strength and porosity is marked. In contrast, in the case of samples made with SA, $CaCO_3$ crystals have no preferential nucleation behaviour and are less likely to nucleate at the interface.

4. Conclusions

Supercritical carbonation of cement-based materials led to significant improvements in porosity and compressive strength. Full carbonation (i.e. complete depletion of C_3S and CH according to XRD) was not necessarily an indicator of good strength development in treated samples as the mix designs played a more critically important role in strength of treated samples. In any case, over the wide range of mix designs studied, all samples were almost fully carbonated after 24hr under supercritical carbonation conditions of 100 bar and 60°C. Samples made without cement (i.e. with a pure lime binder) did not develop significant strength after treatment despite being fully carbonated; the strength of treated samples increased with cement content and full carbonation was not necessary for

16

high strength to be achieved. An interlocking mass of $CaCO_3$ crystals would not appear to be as efficient a binder as a carbonated C-S-H gel phase.

The optimum binder composition with regard to combining high strength and good surface finish was 1:1 lime:cement. The optimum aggregate:binder ratio with regard to treated flexural strength was 2:1. The optimum aggregate composition with regard to treated flexural strength was 65:35 crushed limestone:silica sand. Flexural strengths of >10 MPa were routinely thus achieved.

Treated samples made with crushed limestone exhibited lower porosity, higher strength and better aggregate/matrix interface than those made with silica aggregate. During treatment, the surface of the carbonate aggregate acts to encourage the calcium carbonate fomed during carbonation of CH, unhydrated phases and C-S-H gel to nucleate at the aggregate/matrix interface, encouraging good mechanical bond in the composites. Thus, use of carbonate aggregates in carbonated cementitious composites is likely to lead to superior performance.

References

1. Van Balen K, Van Gemert D. Modelling lime mortar carbonation. Mater. Struct. 1994; 27(7): 393- 398

2. Lawrence RM, Mays TJ, Rigby SP, Walker P, D'Ayala D. Effect of carbonation on the pore structure of non-hydraulic lime mortars. Cem. Concr. Res. 2007; 37(7): 1059-1069.

3. Beruto DT, Barberis F, Botter R. Calcium carbonate binding mechanisms in setting of calcium and calcium magnesium putt limes. J Cult. Herit. 2005; 6(3): 253-260.

4. St Jones DA, Poole AW, Sims I. Concrete Petrography; A handbook of investigative techniques. London: Arnold, 1998.

5. Saetta V, Schrefler BA, Vitaliani RV. The carbonation of concrete and the mechanism of moisture, heat and carbon dioxide flow through porous materials. Cem. Concr. Res. 1993; 23(4):761- 772.

6. Fernandez Bertos M, Simons SJR, Hills CD, Carey PJ. A review of accelerated technology in the treatment of cement based materials and sequestration of CO_2. J. Hazard. Mater. 2004; 112(3):193- 205.

7. Garcia-Gonzalez CA, Hidalgo A, Andrade C, Alonso M C, Fraile J, Lopez-Periago AM, Domingo C. Modification of composition and microstructure of Portland cement pastes as a result of natural and supercritical carbonate procedures. Ind. Eng. Chem. Res. 2006; 45(14):4985-4992.

8. Garcia-Gonzalez CA, Hidalgo A, Fraile J, Lopez-Periago AM, Andrade C, Domingo C. Porosity and water permeability study of supercritical carbonated cement pastes involving mineral additions. Ind. Eng. Chem. Res. 2007; 46(8):2488-2496.

9. Sulapha P, Wong F, Wee TH, Swaddiwudhipong S. Carbonation of concrete containing Mineral admixtures. J. Mater. Civ. Eng. 2003; 15(2):134- 143.

10. Short NR, Purnell P, Page CL. Preliminary investigations into the supercritical carbonation of cement pastes. J. Mater. Sci. 2001; 36(1):35-41.

11. Knopf FC, Roy A, Samrow HA, Dooley KM. High pressure moulding and carbonation of cementitious materials. Ind. Eng. Chem. Res 1999; 38(7): 2641-2649.

12. Neville A M. Properties of concrete. New York: John Wiley & Sons, 1996.

13. Johannesson B, Utgenannt P. Microstructural changes by carbonation of cement mortars. Cem. Concr. Res. 2001; 31(6): 925-931.

14. Purnell P, Short NR, Page C L. Super-critical carbonation of glass fibre reinforced cement Part 1: Mechanical testing and chemical analysis. Composites: Part A 2001; 32(12): 1777-1787.

15. Purnell P, Seneviratne AMG, Short NR, Page CL. Super-critical carbonation of glass fibre reinforced cement Part 2: Microstructural observation. Composites: Part A 2003; 34(11): 1105-1112.

16. Arandigoyen M, Bicer-Simsir B, Alvarez JI, Lange DA. Variation of microstructure with carbonation in lime and blended pastes. Appl. Surf. Sci.2005; 252(20):7562–7571.

17. Van Gerven T, Van Baelen D, Dutre V, Vandecasteele C. Influence of carbonation and carbonation methods on leaching of metal mortars. . Cem. Concr. Res. 2004; 34(1):149- 156.

18

18. Farahi E. Advanced calcareous ceramics via novel green processing and super-critical carbonation. PhD thesis, Warwick, University of Warwick, 2009.

19. Domingo C, Loste E, Gomez-Morales J, Garcia-Carmona J, Fraile J. Calcite precipitation by a high pressure CO_2 carbonation route. J. Supercrit. Fluids 2006; 36(3): 202-215.

20. Onan DD. Effects of supercritical carbon dioxide on well cements, In: Society of Petroleum Engineers of AIME, Editor. Proceeding of the Permian Basin Oil and Gas Recovery Conference. Midland, TX, USA, 1984. p.161-172.

21. Jones RH. Cement treated with high pressure CO_2. US patent 5518540, 21 May 1996.

22. Seneviratne AMG, Short NR, Purnell P, Page CL. Preliminary investigations of the dimensional stability of supercritically carbonated glass fibre reinforced cement. Cem. Concr. Res. 2002; 32(10):1639-1644.

23. Short NR, Brough AR, Seneviratne AMG, Purnell P, Page CL. Preliminary investigations of the phase composition and fine pore structure of super-critically carbonated cement paste. J. Mater. Sci.2004; 39(18): 5683-5687.

24. Aligizaki KK. Pore structure of cement based materials; Testing, interpretation and requirement. Taylor and Francis, 2006.

25. Blyth FGH, De Freitas MH. A geology for engineers. Butterworth Heinemann, 2006.

26. Lye K. Mineral and rocks. A kingfisher guide, London:Ward Lock Ltd, 1979.

27. Al-Kadhimi TKH. Banfill, PFG, Millard SG, Bungey JH. An accelerated carbonation procedure for studies on concrete. Adv. Cem. Res.1996; 8(30): 47-59.

28. Illston JM, Domone PLJ. Construction materials: Their nature and behaviour. Spon Press, 2001.

Table 1

Farahi & Purnell 2012 – Table 1

Table 1: The water content of the mix designs shown in Figure 4, both prior to and post pressing process.

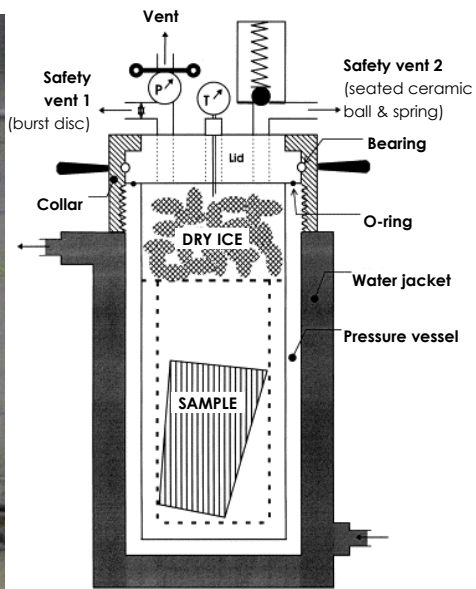| Mix design	Pre-pressing		Post pressing	
A=35:65 CL:S	W/B	W/S	W/B	W/S
0C:0.5L:1A	0.625	0.25	0.51	0.2
0.25C:0.75L:1A	0.55	0.28	0.41	0.21
0.4 C:0.6L:1A	0.50	0.25	0.37	0.18
0.5C:0.5L:1A	0.43	0.21	0.30	0.15
0.5C:0.5L:2A	0.55	0.18	0.31	0.10
0.5C:0.5L:3A	0.68	0.17	0.36	0.09
0.5C:0.5L:4A	0.73	0.15	0.45	0.09
0.5C:0.5L:5A	0.85	0.14	0.53	0.09

Figure 1

Farahi & Purnell 2012 – Figure 1

Figure 2 (revised)
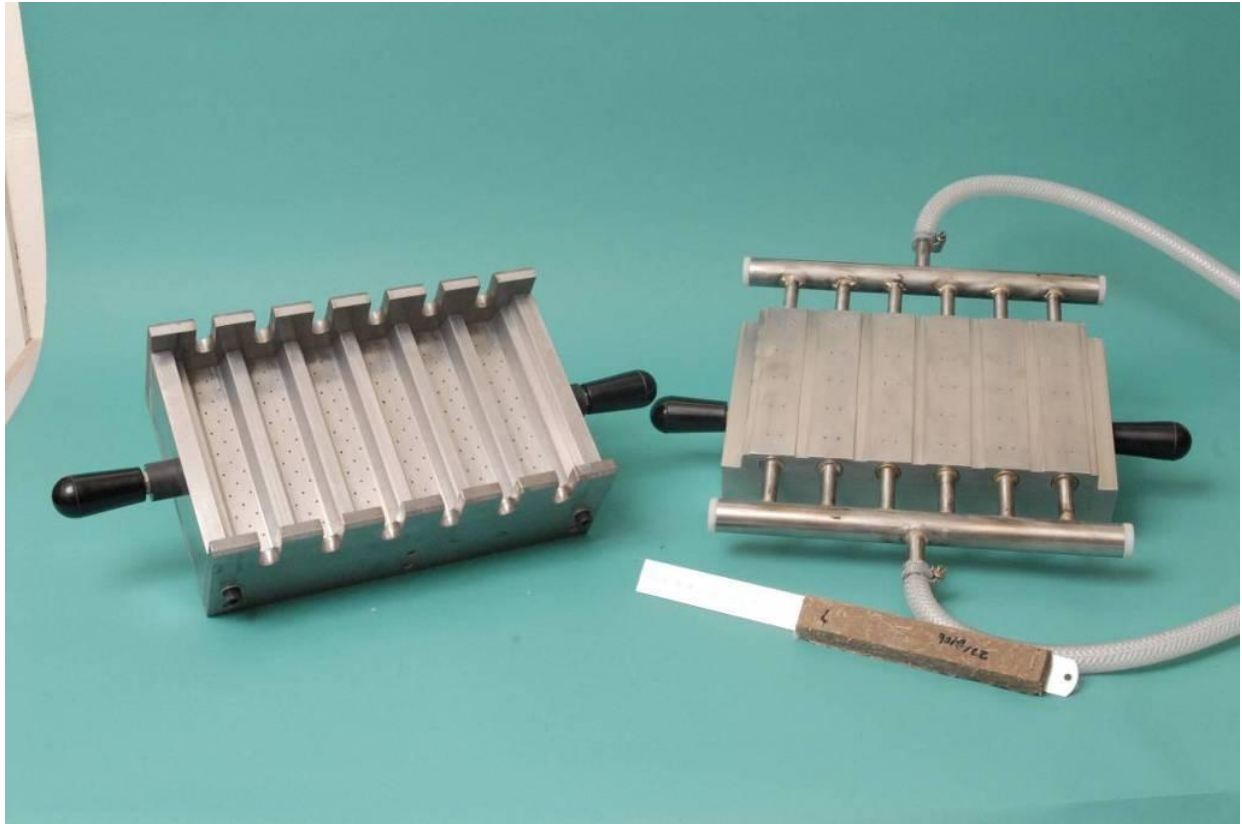
Farahi & Purnell 2012 – Figure 2

Figure 3

Farahi & Purnell 2012 – Figure 3
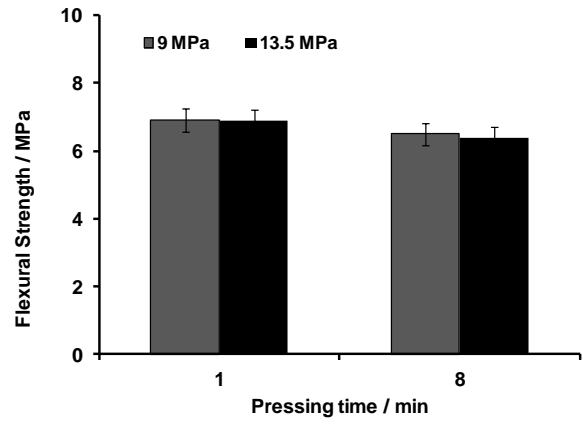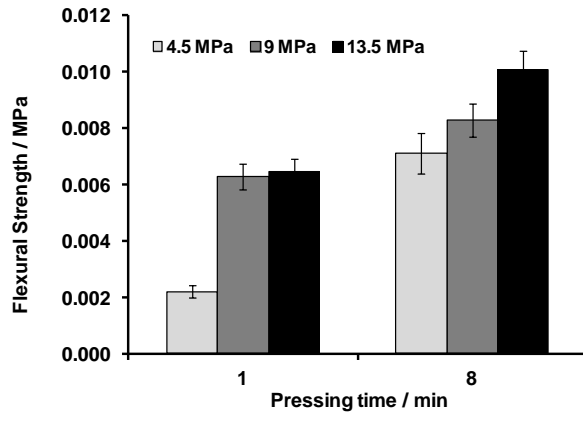
Figure 4

Farahi & Purnell 2012 – Figure 4
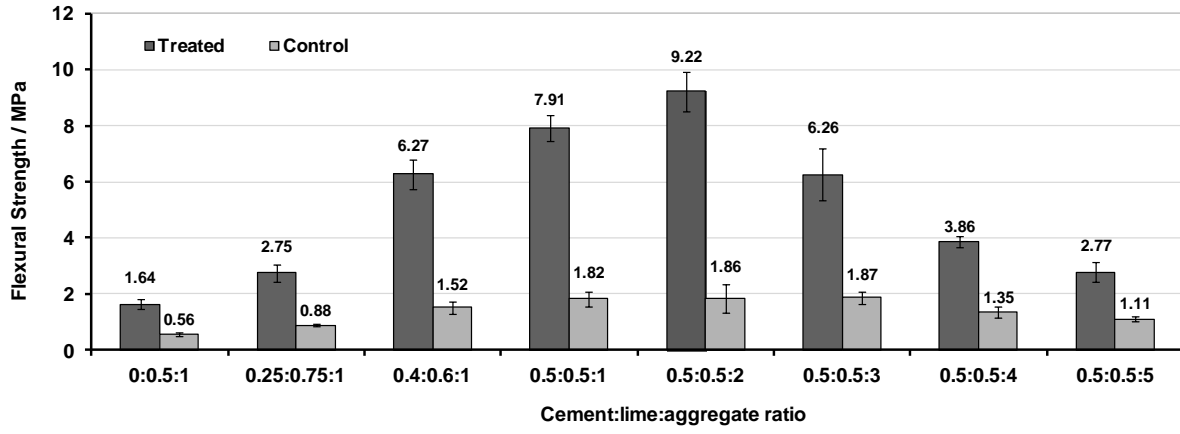
Figure 5

Farahi & Purnell 2012 – Figure 5
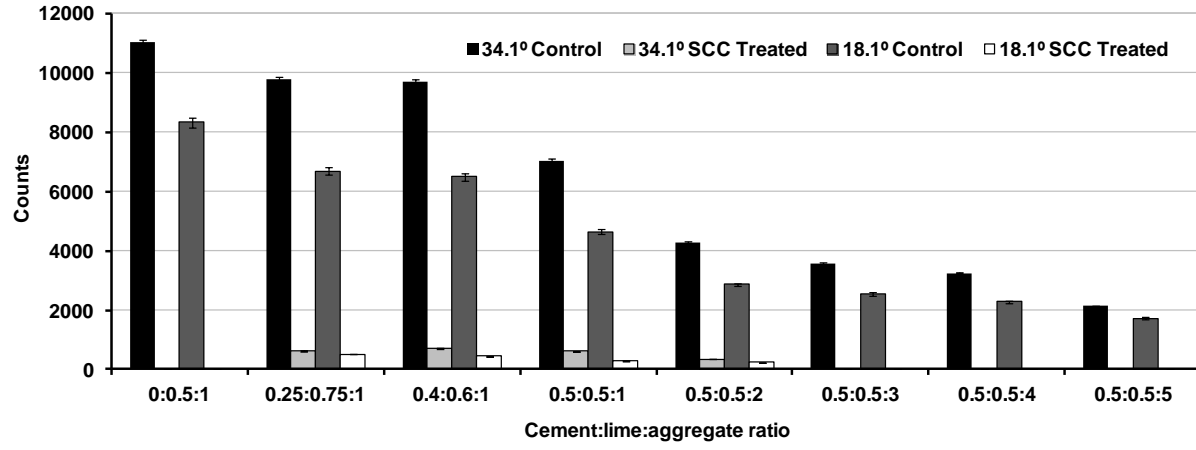
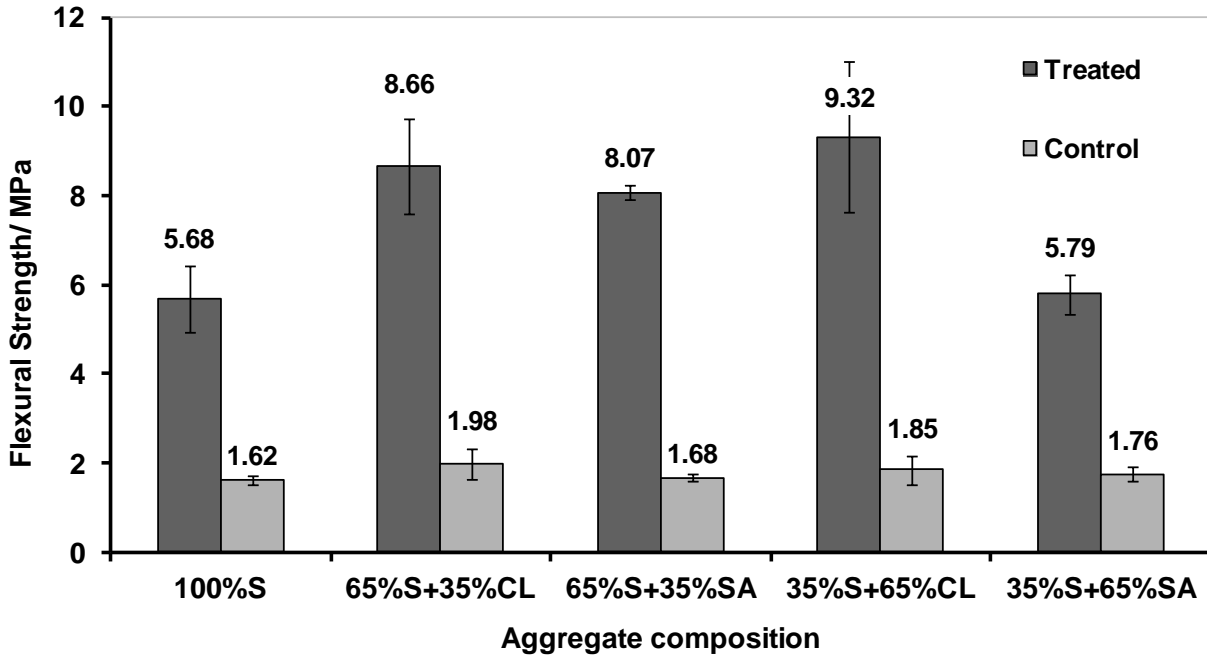**Figure 6**

Farahi & Purnell 2012 – Figure 6
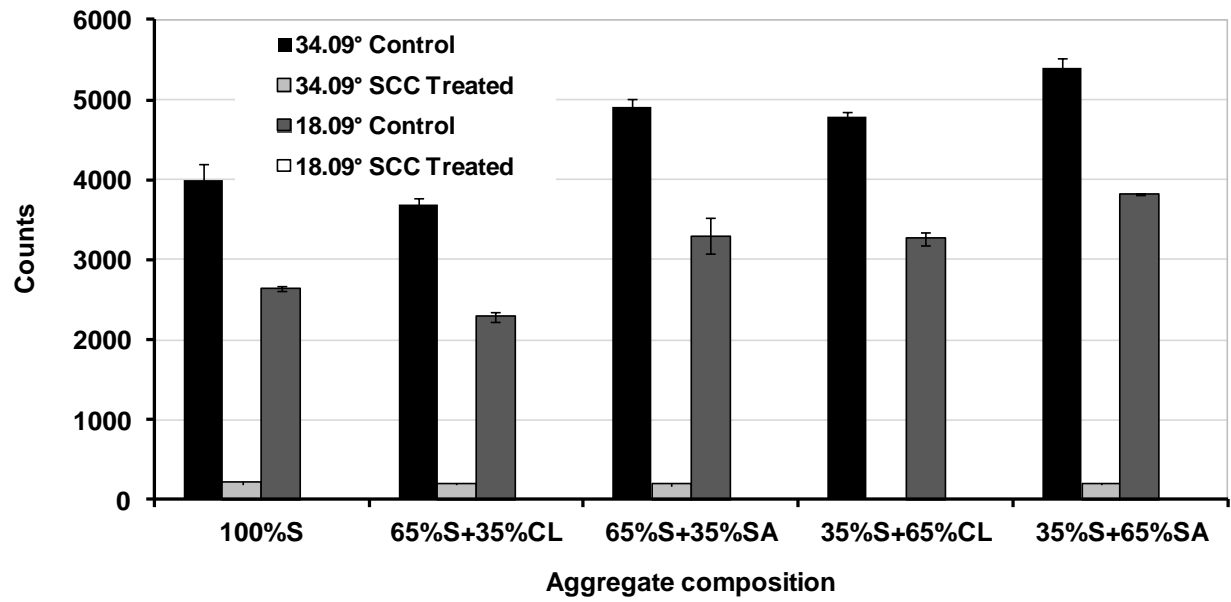
Figure 7

Farahi & Purnell 2012 – Figure 7
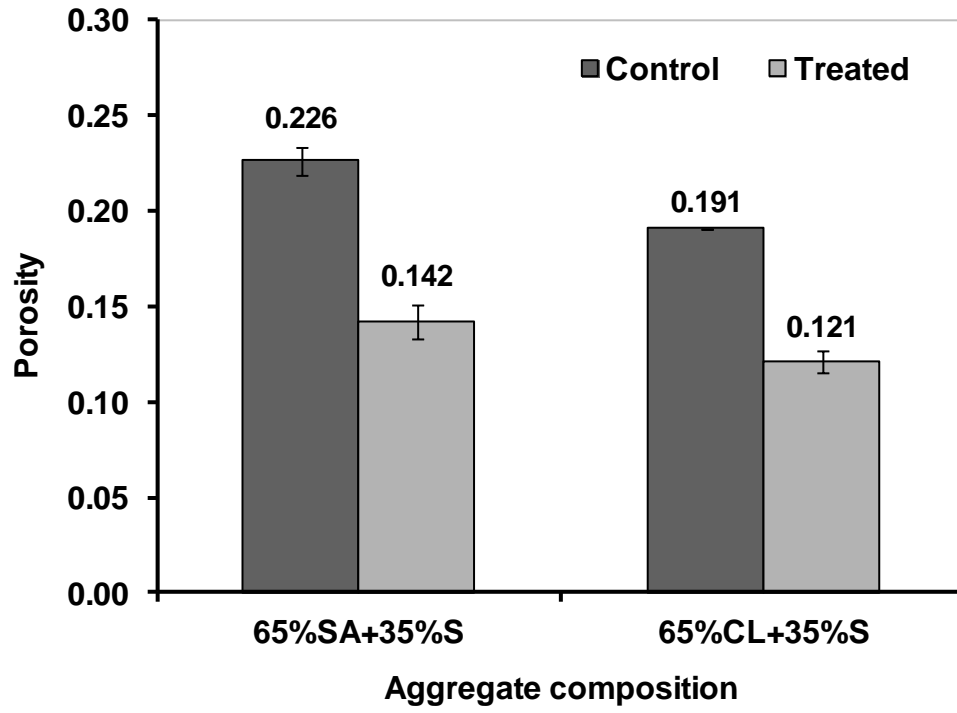
Figure 8

Farahi & Purnell 2012 – Figure 8

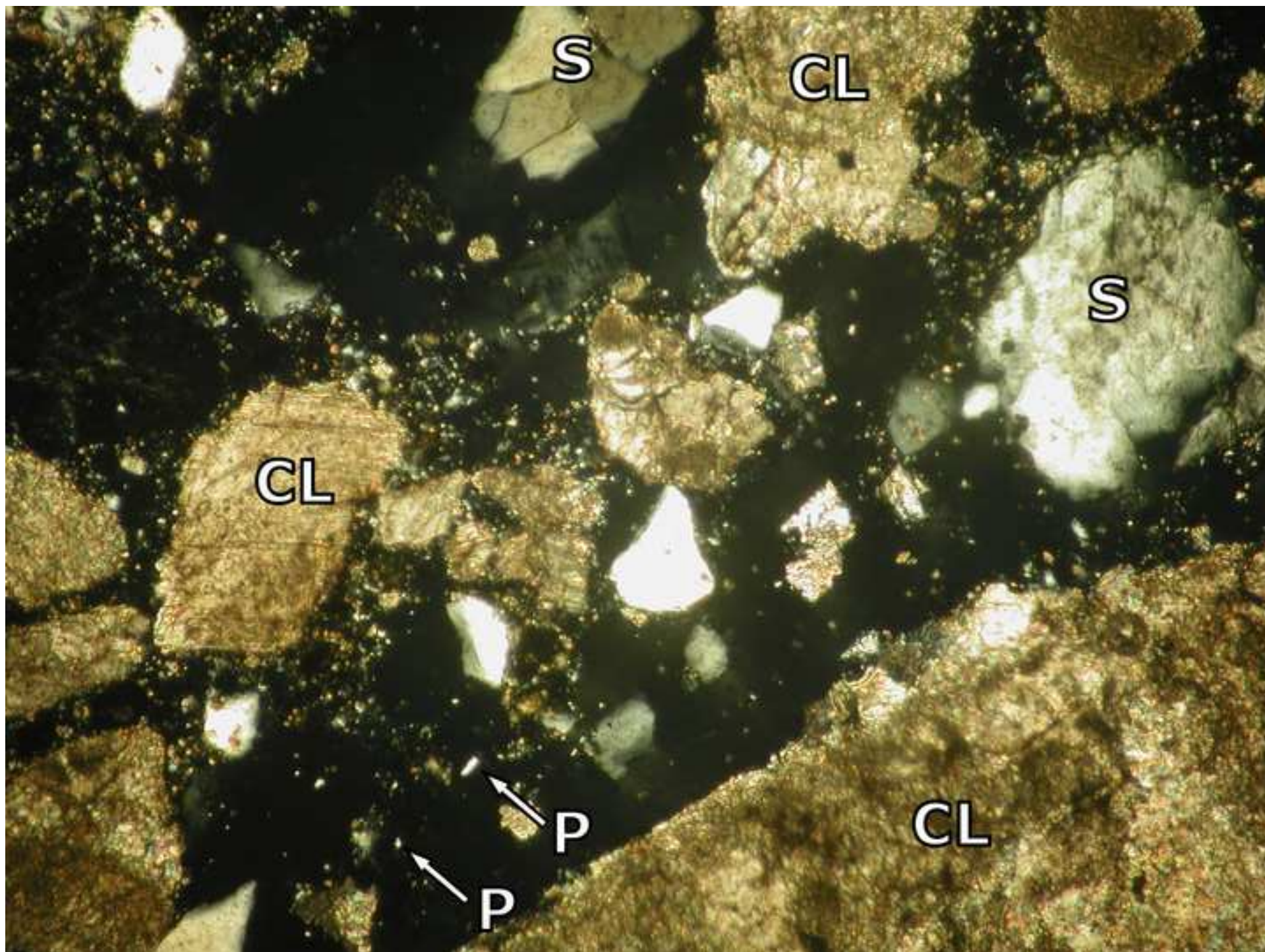**Figure 9**
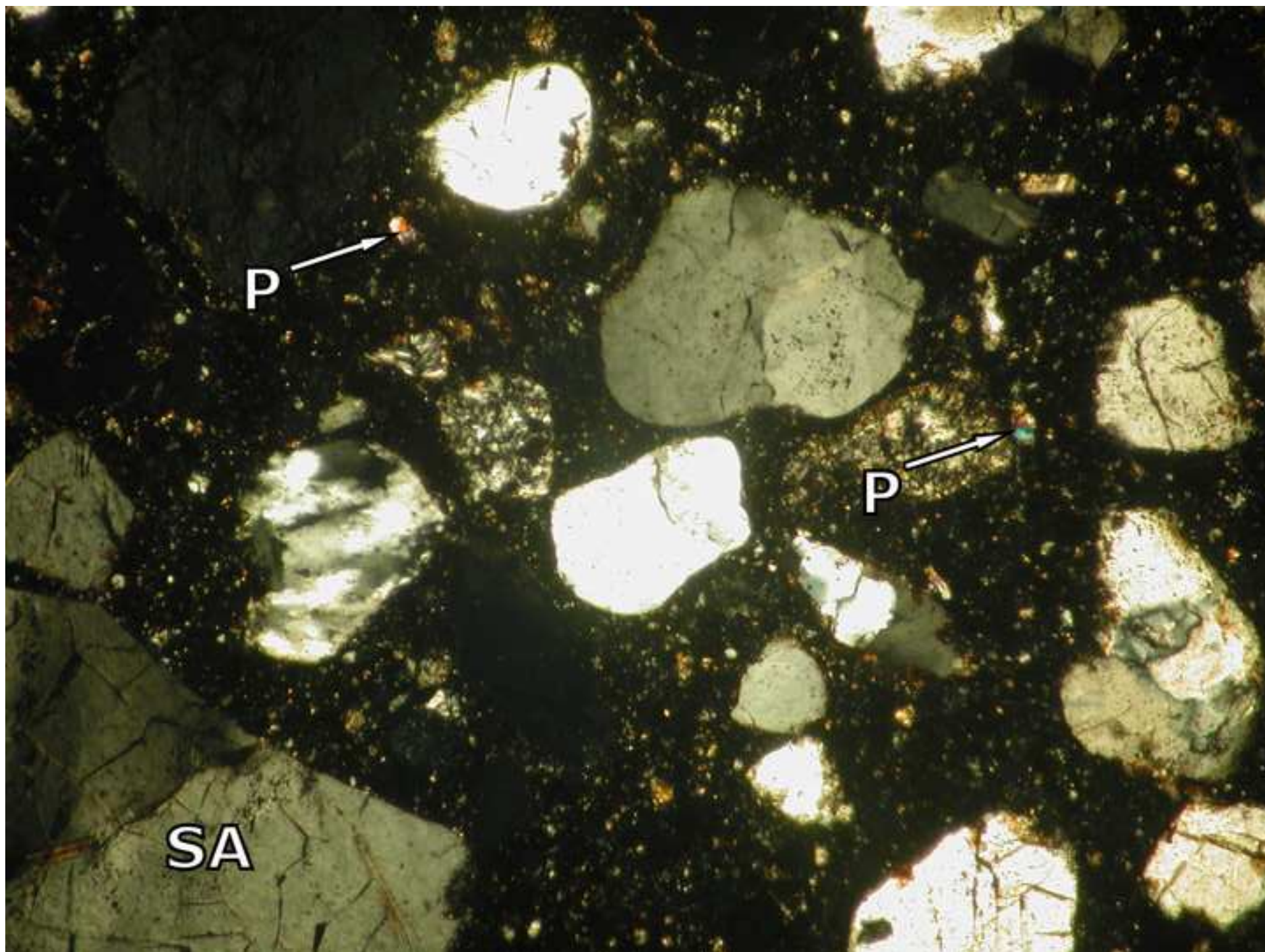**Click here to download high resolution image**

Figure 11
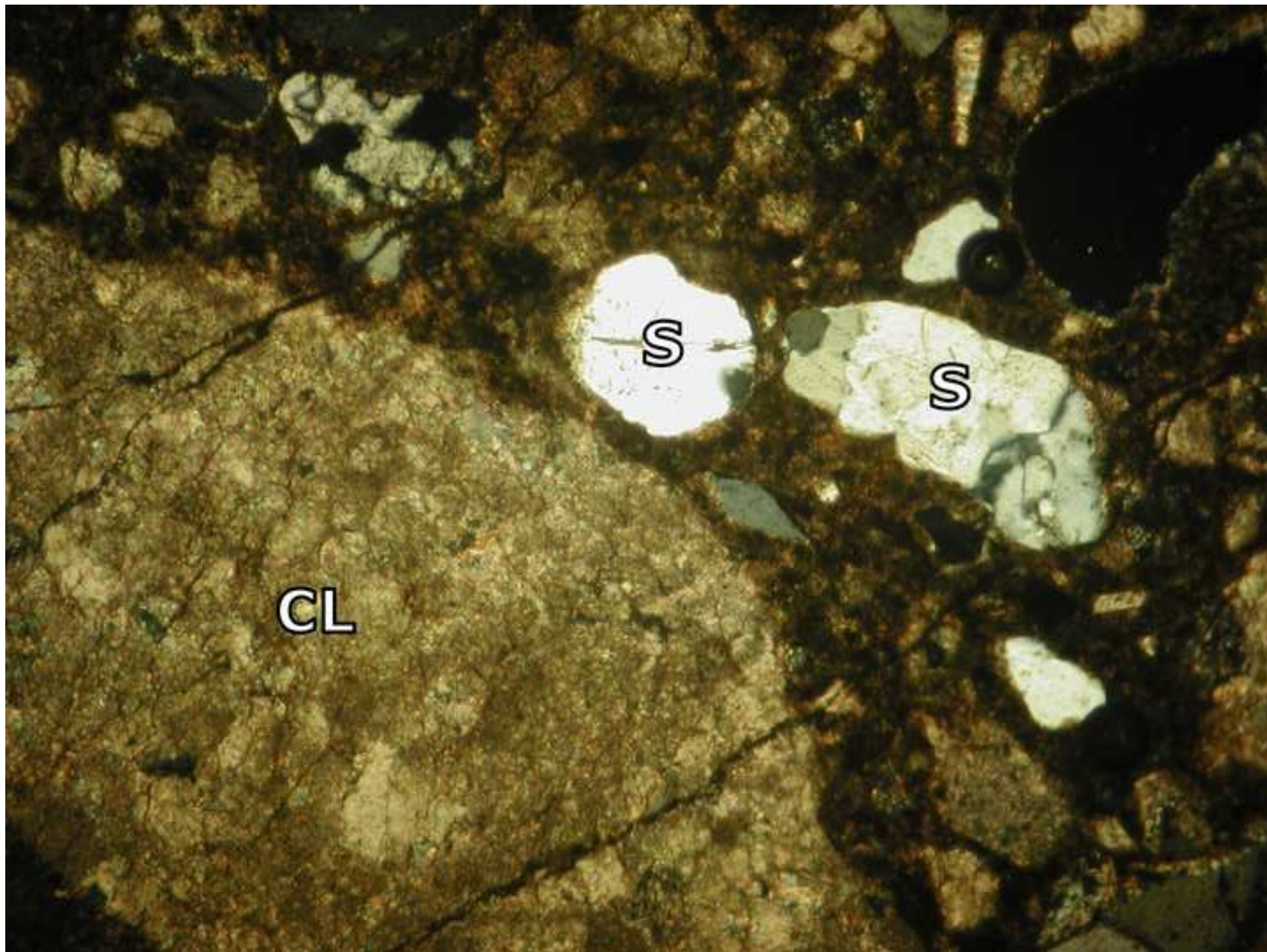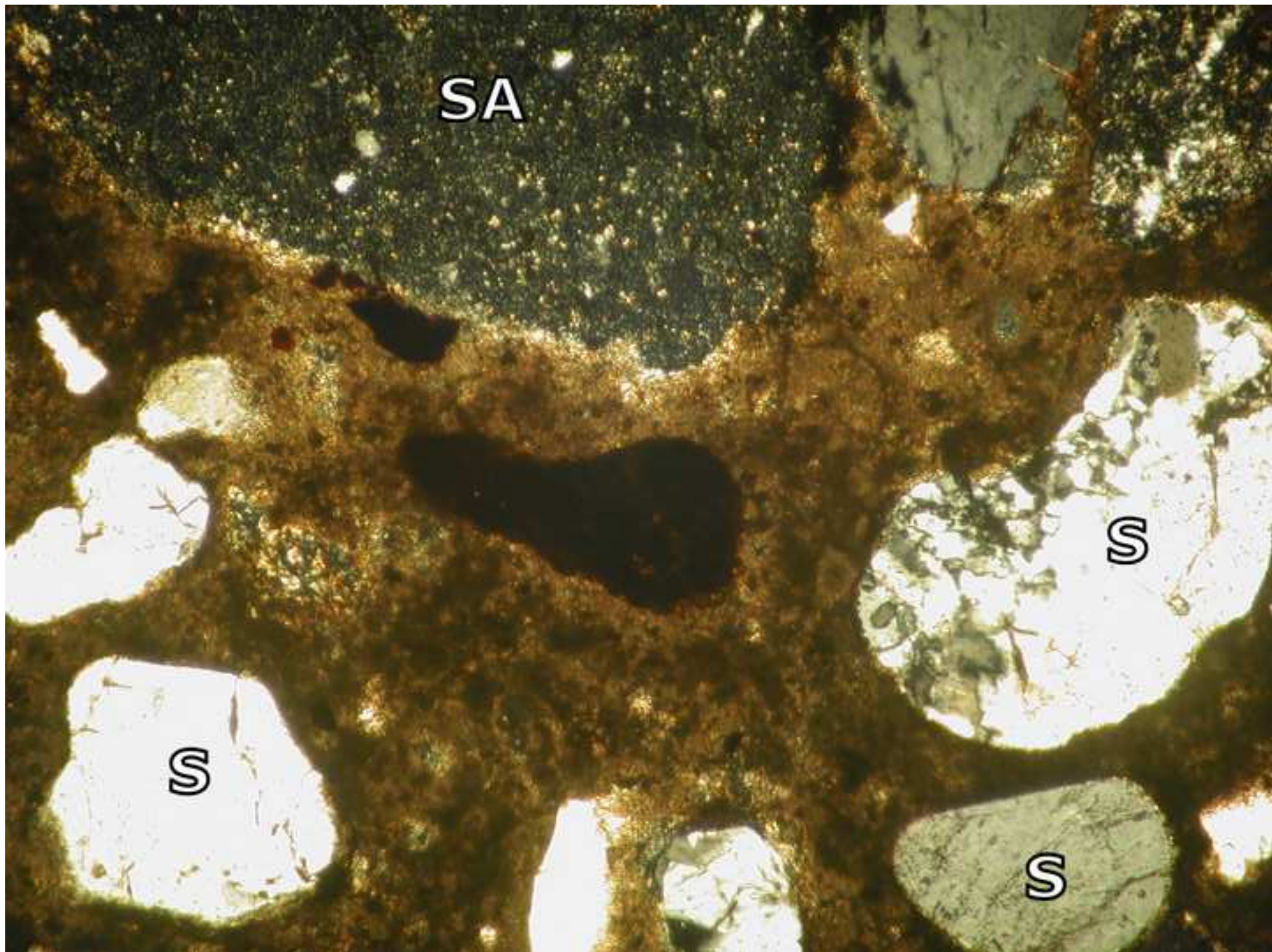[Click here to download high resolution image](#)

Figure 12
[Click here to download high resolution image](#)

Farahi & Purnell 2012 – Figure captions

Figure 1: Compression moulding tool.

Figure 2: Photo and diagram illustrating the $scCO_2$ reaction vessel

Figure 3: Processing parameters vs flexural strength. Left: green samples; right: carbonated samples. Legend = compression moulding pressure. Error bars = ± 1 st dev.

Figure 4: Flexural strength vs. mix design. Aggregate = 35:65 S:CL. All proportion ratios by mass. Error bars = ± 1 st dev.

Figure 5: XRD analysis of CH depletion vs. mix design. Aggregate = 35:65 S:CL. All proportion ratios by mass. Error bars = ± 1 st dev.

Figure 6: Flexural strength vs. aggregate composition. Mix design 0.5C:0.5L:2A . All proportion ratios by mass. Error bars = ± 1 st dev.

Figure 7: XRD analysis of CH depletion vs. mix design. Mix design 0.5C:0.5L:2A. All proportion ratios by mass. Error bars = ± 1 st dev.

Figure 8: Porosity (via helium pycnometry) vs aggregate composition. Mix design 0.5C:0.5L:2A. All proportion ratios by mass. Error bars = ± 1 st dev.

Figure 9: Thin section micrograph of control sample with crushed limestone aggregate (A = 65:35 CL:S). Horizontal field of view = 0.7 mm. Cross-polarised light. P = portlandite $Ca(OH)_2$

Figure 10: Thin section micrograph of control sample with silica aggregate (A = 65:35 SA:S). Details as figure 9.

Figure 11: Thin section micrograph of SCC treated sample with crushed limestone aggregate (A = 65:35 CL:S). Details as figure 9.

Figure 12: Thin section micrograph of SCC treated sample with silica aggregate (A = 65:35 SA:S). Details as figure 9.